Vapor Pressure of Silicon Monoxide

Frank T. Ferguson*,† and Joseph A. Nuth III‡

Code 691, NASA-Goddard Space Flight Center, Greenbelt, Maryland 20771, and Department of Chemistry, Catholic University of America, Washington, D.C. 20064

Silicon monoxide is a material that is used extensively in the glass and metallurgical industries. In addition, silicon monoxide is also particularly important to the field of astrophysics where it is theorized to play a vital role in the production of metal silicate dust grains in the condensing outflows of dying stars. In this work, the evaporation coefficients and vapor pressure of commercially available amorphous silicon monoxide were measured over the temperature range (1301 to 1519) K using a Knudsen effusion cell and a commercial, thermogravimetric balance. A second- and third-law analysis of the vapor pressure data yielded (351 ± 11) and (359.1 ± 2.0) kJ·mol^{-1} for the enthalpy of the vaporization reaction at 298.15 K, respectively. It is also shown that a thermodynamic assessment of silicon monoxide vapor pressure that has been used in the modeling of astrophysical condensation at 1000 K and below greatly overpredicts silicon monoxide vapor pressure.

1. Introduction

Silicon monoxide is a substance that is important in a variety of fields including the metallurgical and glass industry, in the production of optical coatings, and in the production of large silicon monocrystals in the semiconductor industry. Recently, thin films of Al:SiO prepared from the condensation of gaseous SiO have been used to produce light-emitting diodes, and other optical devices are envisioned using this process.[1] The thermodynamic properties of SiO are also vital in the modeling of silicate dust grain formation in astrophysical scenarios. Based on its large solar abundance, silicon monoxide has long been suggested as a possible initial condensate in the outflows from oxygen-rich dying stars. In addition, observations of the dust shells around these stars indicate the presence of silicate grains, some of which are crystalline, at temperatures in excess of 1000 K. This observation places an important constraint on modeling of grain formation via SiO condensation in these circumstellar dust shells. Namely, these silicates must occur via homogeneous nucleation above 1000 K or by heterogeneous growth on pre-existing seed nuclei of some other refractory species. In spite of its high relative abundance, current models of SiO nucleation indicate that SiO does not condense at an appreciable rate via homogeneous nucleation until approximately 600 K.[2−5]

The properties of silicon monoxide have been the subject of debate for many years. Amorphous silicon monoxide can be produced by condensing the vapors over a mixture of Si and SiO_2 at elevated temperatures and commercially available SiO is, in fact, made in a similar fashion. This reaction is reversible and the amorphous SiO disproportionates to form Si and SiO_2, though the rate at which this occurs will of course depend upon the temperature.[6] In their assessment of the properties of SiO, Kubaschewski et al. speculated that $SiO_{(am)}$ could be stable above 1373 K.[7] According to Nagamori, this lower stability temperature for SiO appears to be in the range from (1173 to 1273) K, based on recent observations.[8] Still, other works suggest that $SiO_{(am)}$ is unstable at all temperatures below 1723 K.[9] Hertl and Pultz have measured this disproportionation reaction by heating samples of SiO under vacuum or argon and measuring the rate of production of silicon with time.[6] In addition to quantifying this reaction rate, they also found that this disproportionation reaction is not limited to the surface layers and occurs throughout the bulk.

In addition to the question of stability, for many years there has also been a debate over whether "SiO" itself is a pure compound, i.e., silicon(II) oxide, or simply a stoichiometric mixture of Si and SiO_2. In the random-bonding (RB) model of SiO, silicon−silicon and silicon−oxygen bonds are theorized to be randomly distributed throughout the material.[10] In the random-mixture (RM) model, it is speculated that over certain small domains, silicon is bonded to only silicon or oxygen, corresponding to an intimate, two-phase mixture of Si and SiO_2.[11] In recent years, experimental evidence taken via various methods including X-ray photoelectron spectroscopy (XPS),[1,12] electron scattering and electron energy-loss spectroscopy (EELS)[9] and X-ray absorption near edge structure (XANES)[13] have confirmed that silicon(II) oxide does not exist as a distinct phase but as a mixture of Si and SiO_2, more in line with the RM model. The interface for this mixing occurs over the scale of (3 to 4) nm. Therefore, as noted by Schnurre et al., amorphous SiO is not a classical homogeneous single phase, yet because of this small domain size it is also not a classical heterogeneous two-phase mixture.[9]

As noted earlier, silicon monoxide vapor is produced by heating either (nominally) amorphous silicon monoxide

$$SiO_{(am)} \rightarrow SiO_{(g)} \quad (1)$$

or mixtures of silicon and silica

$$\frac{1}{2}Si_{(cr)} + \frac{1}{2}SiO_{2(s)} \rightarrow SiO_{(g)} \quad (2)$$

Throughout this work, the SiO_2 is assumed to be in the form of high cristobalite. While the number of vapor pressure studies of both of these reactions is very limited, the number of studies

* To whom correspondence should be addressed. E-mail: frank.ferguson@nasa.gov.
† Catholic University of America.
‡ NASA-Goddard Space Flight Center.

10.1021/je800560b CCC: $40.75
Published on Web 10/31/2008

of eq 2 outweigh those of reaction 1. One complication in both of these evaporation reactions is that they both have low evaporation coefficients. Gunther studied both of these reactions and found evaporation coefficients for the $SiO_{(am)}$ reaction to be approximately 1/20 while the evaporation coefficient for reaction 2 was approximately an order of magnitude less.[14] These low evaporation coefficients for both reactions have made a proper interpretation of silicon monoxide vapor pressure difficult. In 1992, Rocabois et al. performed twin Knudsen cell effusion studies of both reactions 1 and 2 and measured the evaporation coefficients for both.[15] Their work agreed with Gunther's observations, underscoring the need to consider these low evaporation coefficients in such studies. Furthermore, when the evaporation coefficients were properly taken into account, Rocabois et al. showed that the silicon monoxide vapor pressure for either reaction 1 or 2 was identical within the expected uncertainty of their measurements.

Due to the small number of vapor pressure studies on amorphous SiO and to help answer some of the questions regarding the thermochemical properties of SiO, the goal of this work is to provide vapor pressure data for (nominally), amorphous SiO. These data were collected using a typical Knudsen cell and a commercial thermogravimentric balance.

2. Experimental Apparatus

A brief overview of the experimental equipment is given in this section. More detail regarding both the equipment used and the experimental procedure can be found in recent measurements of the vapor pressure of iron and palladium.[16,17]

The experimental apparatus consists of a commercial thermogravimetric balance used to measure the rate of mass loss from a Knudsen cell. A cross-sectional diagram of the experimental apparatus is shown in Figure 1. The balance is capable of measuring sample masses up to 100 g with microgram sensitivity at temperatures up to 1973 K. Samples are suspended on one arm of the balance using a hangdown assembly. During runs the sample cell is placed within the alumina reactor tube which is centered within the resistive furnace section of the device. Six molybdenum disilicide heating elements are equally spaced around this tube and a long, alumina-sheathed, type-B thermocouple is used to measure the cell temperature and for furnace control. During a run, the lower section of the Knudsen cell is centered within the furnace area and the thermocouple is positioned approximately 5 mm from the bottom of the sample cell. During operation, the balance assembly and the furnace reactor tube are evacuated using the combination of a mechanical and turbomolecular pump. Vacuum level within the reactor tube is maintained at 10^{-3} Pa or better.

The Knudsen cell used in this work is identical to that used with palladium and a representation of this cell is shown in Figure 2. The cell is approximately 5.5 cm in height with an outer diameter of 1.27 cm and is constructed from two, closed-end, 99.8 % alumina tubes. One tube has an outside diameter just slightly smaller than the inside diameter of the second tube. The cell is constructed by inverting the smaller tube and placing it within the larger tube. An effusion orifice is drilled through the smaller tube sidewall using diamond-coated drill bits and this orifice is positioned in a window through the larger tube as shown in Figure 2. The use of tubes in this inverted fashion greatly reduces the possibility of vapor escaping from areas other than the effusion orifice. Nevertheless, the seams along the top and along the "window" of the larger tube are additionally sealed with a zirconia-based cement (Resbond 904, Cotronics Corp.). Care was taken to use the minimum amount of this cement necessary to seal these seams. Once the cell is constructed, it is attached to the hangdown assembly of the balance arm using an alumina pin. It should be noted that all parts of the cell and the hangdown assembly in the furnace hot zone are made entirely of 99.8 % alumina with the exception of the small amount of zirconia adhesive.

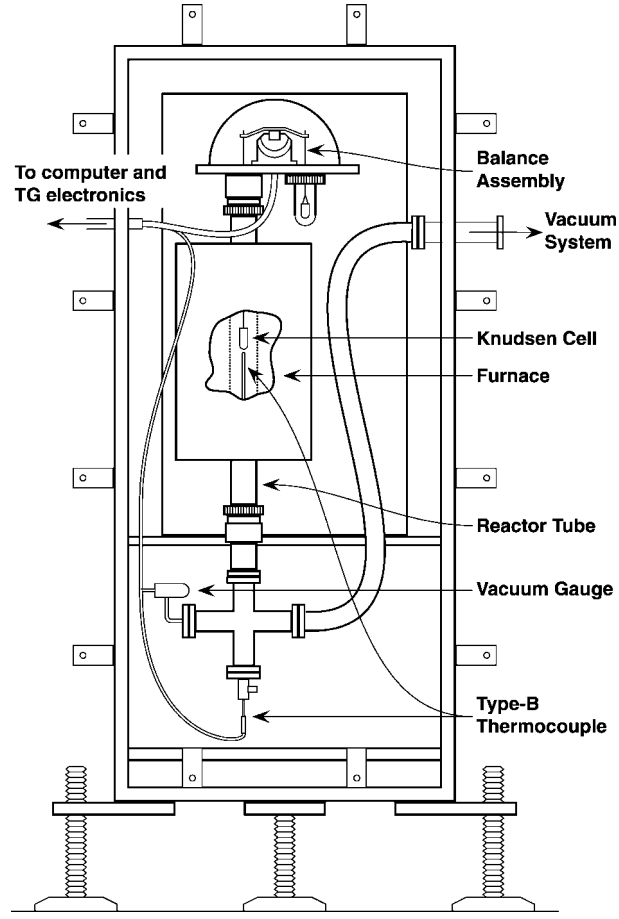

Figure 1. Schematic diagram of thermogravimetric balance and furnace assembly.

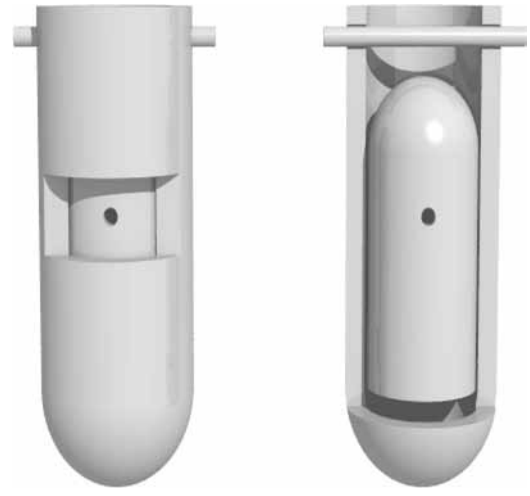

Figure 2. Alumina effusion cell constructed from two closed-end tubes.

3. Experimental Procedure

The first step in an experimental run is the construction of the sample cell. When completed, the cell is filled with commercial SiO powder (Alfa, 99.9 % optical grade, 120 mesh)

and sealed. The orifice diameter is measured using an optical microscope and traveling stage of micrometer accuracy as described in an earlier paper.[16] The cell is then placed on the balance arm, and the reactor tube and balance volume are evacuated. In the case of SiO, the cell was pumped under vacuum for 24 h at room temperature before a run. The sample was then heated to the desired temperatures, and the mass of the sample cell was continously monitored, taking temperature and mass measurements twice per second.

In the same manner as was done for palladium, after a run, 2 min averages of the resulting large data set were taken of both the temperature and mass datapoints. These data were then processed by a computer program to calculate the mass loss rates as a function of temperature. In this program, the temperature data were searched for regions where the temperature remained essentially constant. For these isothermal periods, the rates of mass loss were constructed from these 2 min averages. All of these values for an isothermal period were averaged and the standard deviation of this mean value was then used as an estimate of the uncertainty in this mass loss rate and used in the calculation of the vapor pressure.

4. Vapor Pressure Calculation

The measured vapor pressure, P_m, is related to the mass loss rate, $\dot{m}$, via the Hertz−Knudsen equation:

$$P_m = \frac{\dot{m}}{W_B B}\sqrt{\frac{2\pi RT}{M_w}} \tag{3}$$

where B is the cross-sectional area of the effusion orifice, R the gas constant, T the temperature of the gas, and M_w the molecular weight of the effusate. The term W_B is the Clausing correction factor for the cell orifice. If the cell wall thickness is knife-edge thin, this factor is 1.0. If, as is typical, the wall in the vicinity of the orifice has some finite thickness, this short "pipe" can cause an impedance to the transmission of molecules from the cell. This factor, W_B, accounts for this back-reflection of some of the molecules and is based on the work of Clausing.[18] For arbitrary geometries, this factor must be computed from the Clausing integral equation. Berman developed a series expansion approximation to this equation for capillaries and this formula has been used to calculate the Clausing factors for the cell.[19] For an effusion orifice of radius, a, and wall thickness ("pipe" length), l, the Clausing coefficient, W, is given by

$$W = Q_1 - Q_2 \tag{4}$$

where

$$Q_1 = 1 + (L^2/4) - (L/4)(L^2+4)^{1/2} \tag{5}$$

$$Q_2 = \frac{[(8-L^2)(L^2+4)^{1/2} + L^3 - 16]^2}{72L(L^2+4)^{1/2} - 288\ln[L + (L^4+4)^{1/2}] + 288\ln 2} \tag{6}$$

and

$$L = l/a \tag{7}$$

The accuracy of this equation has been verified by Monte Carlo simulations[20] and this expression is reported to be better than 0.1 % for $0 \le L \le 5$, a range common to Knudsen effusion studies.[21]

As noted in the Introduction, silicon monoxide is expected to have a low evaporation coefficient. Whitman and Motzfeldt developed the following equation to account for such low evaporation coefficients in Knudsen cells:[22,23]

$$P_{eq} = \left[1 + f\left(\frac{1}{\alpha} + \frac{1}{W_A} - 2\right)\right]P_m \tag{8}$$

In this equation, the impedance of the flow of molecules to the effusion orifice height is included in the term given by W_A, the Clausing factor for the cell. The term P_{eq} is the true equilibrium vapor pressure, α is the evaporation coefficient, and the term f is a factor related to the cell geometry and is given by

$$f = \frac{W_B B}{A} \tag{9}$$

where A is the cross-sectional area of the evaporating surface.

In experiments with low evaporation coefficients, this value, α, can be estimated by rearranging eq 8 to

$$P_m = P_{eq} - P_m f\left(\frac{1}{\alpha} + \frac{1}{W_A} - 2\right) \tag{10}$$

Therefore, if a series of effusion experiments are made with different orifice sizes, and the data are plotted on a graph as P_m vs $P_m f$ and fitted to a straight line, the resulting intercept should yield the equilibrium vapor pressure, P_{eq}, while the value of the evaporation coefficient, α, may be computed from the slope.

5. Estimation of Experimental Uncertainties

The cell and experimental apparatus used in this study are identical to those used for a recent study with palladium and the estimated uncertainties in the measured observables are essentially identical to those of that study.[16] The molecular weight for SiO was taken as 44.0849 from the NIST-JANAF thermochemical tables.[24]

The experimental uncertainty in the type-B thermocouple used to measure the furnace and cell temperature is expected to be ± 5 K. To test the accuracy of the thermocouple, the measured furnace temperature was compared against the melting point of copper. A differential thermal analyzer (DTA) system was constructed using graphite crucibles. Two junctions of a type-K thermocouple were wired in series, with the negative leads tied together. Each of these junctions were then connected to one of the two graphite crucibles. If the two crucibles are at the same temperature, the voltage generated in one thermocouple circuit will be equal and opposite to the voltage generated by the second thermocouple circuit, resulting in no net voltage at the terminal ends of the circuit. If there is a temperature difference between these two crucibles, there will be a net voltage, either negative or positive, measured at the circuit terminals. A small sample of pure copper was placed in one crucible while a sample of molybdenum was placed in the other. The DTA assembly was similar in size to the Knudsen cells used to measure vapor pressure and was placed in the same location as used in the vapor pressure measurements. The furnace was then cycled above and below the known melting point of copper at various heating rates.

Shown in Figure 3 are the recorded temperature differences between the two crucibles as a function of the measured furnace temperature. In this figure, positive differences in temperature represent melting of the copper sample, while the negative deviations indicate solidification of the sample. The two vertical, dashed lines represent ± 5 K deviations about the true melting point of copper, 1357.77 K. The curves with the highest recorded changes in temperature correspond to a heating rate of approximately 5 $K \cdot min^{-1}$ while the lowest deviations occur at a heating rate of 0.1 $K \cdot min^{-1}$. As shown in Figure 3, the observation of the copper fusion temperature is very repeatable. As the heating and cooling rates are decreased, the temperature

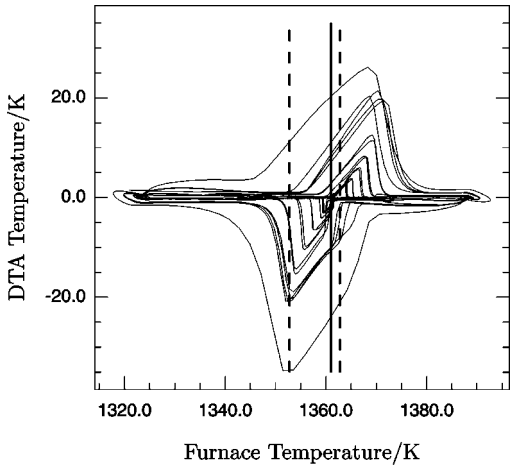

Figure 3. Test of the furnace thermocouple accuracy. A differential thermal analyzer (DTA) was used to measure the fusion temperature of a copper sample at different heating rates. The solid vertical line denotes the measured fusion temperature while the vertical, dashed lines represent ± 5 K region about the true fusion temperature of copper.

deviations due to melting and solidification converge to the temperature denoted by the solid, vertical line. This temperature is close to the midpoint of the experimental temperature range for the SiO vapor pressure taken in this work and also falls within the ± 5 K bands about the copper fusion temperature denoted by the dashed vertical lines. Therefore, the estimated uncertainty in all temperature measurements is taken to be ± 5 K.

The mass loss rates are calculated via the averaging procedure explained in the previous section. The standard deviation of these mean mass loss rates are used as an estimate of the uncertainty in these quantities. This uncertainty only reflects the variation in the mass loss due to fluctuations in the balance signal. Winterbottom and Hirth have demonstrated that in some cases surface diffusion can contribute to a much higher flux from a Knudsen cell and, if not included in the analysis of the data, can lead to an apparently higher vapor pressure.[25] This contribution is especially large in the case of a knife-edged orifice. Unfortunately, this additional surface diffusive flux depends on quantities that are typically unavailable or poorly known. Ward et al. performed a Monte Carlo analysis corroborating the work of Winterbottom and Hirth.[26] Ward et al. also provided a fit to their data that could be used to account for the surface diffusive contribution if the mean surface diffusion distance, $\bar{x}$, is known. This value typically ranges between (0 and 0.02) cm. Using an estimate of 0.01 cm for this value and the actual Knudsen cell geometry from this work, the maximum difference in the computed vapor pressures would be approximately 3 % or less. Since the information needed to accurately compute and account for this contribution to the flux is not available and the expected influence in the results is less than that expected from the other experimental uncertainties, this contribution is neglected.

The Knudsen orifice diameter is measured using the microscope and stage assembly described earlier, and it is estimated that the uncertainty in this value is ± 0.02 mm. Likewise, the wall thickness at each orifice is measured at the same level of uncertainty as (1.27 ± 0.02) mm. To calculate the Clausing factor for the cell, information about the geometry of the cell interior must be known. These interior conditions are, of course, less precisely known. Fortunately, the calculations of the equilibrium vapor pressure are also less sensitive to these values. The estimated height from the evaporating surface to the effusion orifice is estimated to be (10 ± 2) mm while the evaporating surface is estimated to be simply the cross-sectional area of the cell. This area is caluclated based on an estimated cell internal diameter of (6.3 ± 0.2) mm.

The contributions from all of the aforementioned uncertainties are considered in assigning the final uncertainty value to the calculated equilibrium vapor pressure. For example, if the uncertainties in the temperature, orifice diameter, and mass loss rate are denoted by δT, δd, and $\delta \dot{m}$, respectively, then the uncertainty δq, in a derived quantity, q, is given by

$$\delta q = \left\{ \left[\left(\frac{\partial q}{\partial T} \right) \delta T \right]^2 + \left[\left(\frac{\partial q}{\partial d} \right) \delta d \right]^2 + \left[\left(\frac{\partial q}{\partial \dot{m}} \right) \delta \dot{m} \right]^2 \right\}^{1/2} \quad (11)$$

As in the case of the previous work with palladium, the two dominant sources of error are the uncertainty in the mass loss rate and in the determination of the orifice diameter. In most cases, the uncertainty in the mass loss rate is rather small. Nevertheless, there are some points, particularly at the low effusion rates at the lower temperatures, where the fluctuations in the mass loss rates are larger than typical and contribute to higher uncertainty limits for these vapor pressure values.

6. Results

Data for SiO evaporation were taken using three cells of different effusion orifice diameters: 1.15 mm, 1.34 mm, and 1.76 mm. Listed in Table 1 are the run temperature, the diameter of the cell orifice, the area of the effusion orifice, the Clausing factor for the orifice, the area of the evaporating surface, the Clausing factor for the cell, the total mass lost during the isothermal period, the duration of the isothermal period, the computed loss rate and its estimated uncertainty, the factor, f, as given by eq 9 for each cell, and the value of P_m as given by eq 3 for each run. It should be noted that the mass loss rate is calculated via the averaging procedure described earlier and is not calculated simply from the total mass loss rate and loss time as given in Table 1, though the two values should be extremely close. In addition, these mass loss rates are only computed for the isothermal periods and do not include mass losses during the dynamic temperature ramps before and after these isothermal plateaus.

As noted earlier, the goal in each of these individual experiments is to use data taken at a fixed temperature to construct plots of P_m vs ($P_m f$). The 42 data points from the three cells cover the temperature range from (1301 to 1519) K. As shown in Table 1, the values of P_m exhibit different values of uncertainty and this is based on experimental conditions such as the measured mass loss rate. Therefore, a plot of P_m vs ($P_m f$) for different cell sizes would be subject to varying uncertainty in both the x and y coordinates. Therefore, a linear fit to the data was made using the FITEXY routine that provides a weighted linear fit to data when there are uncertainties in both coordinates.[27] Weighting factors, w_i, were constructed from the estimated uncertainties, σ_i, using the following formula:

$$w_i = 1/\sigma_i^2 \quad (12)$$

In addition to the fit parameters, this routine also provides uncertainty estimates in these parameters and these have been used to compute the uncertainty estimates in the final results. The results of these fits are given in Table 2. The values for the evaporation coefficient, α, and its associated uncertainty are given in the second column of the table. Over the experimental temperature range, these values range from approximately 0.02 to nearly 0.05, increasing in value with increasing temperature. In 1992, Rocabois et al. reported results of a study of $SiO_{(am)}$

Table 1. Experimental Data for SiO Vapor Pressure Measurements[a]

T/K	d/mm	B/cm^2	W_B	A/cm^2	W_A	m/mg	t/s	$\dot{m}$(mg·min^{-1})	f	P_m/Pa
1301	1.15	0.0103	0.491	0.317	0.412	3.36	28500	0.0071 ± 0.0005	0.016	0.29 ± 0.03
1301	1.34	0.0140	0.526	0.317	0.412	4.89	28500	0.010 ± 0.002	0.023	0.29 ± 0.05
1301	1.76	0.0243	0.588	0.317	0.412	2.04	11100	0.011 ± 0.001	0.045	0.16 ± 0.02
1315	1.15	0.0103	0.491	0.317	0.412	2.23	13800	0.0097 ± 0.0005	0.016	0.40 ± 0.03
1315	1.34	0.0140	0.526	0.317	0.412	3.28	13800	0.014 ± 0.002	0.023	0.40 ± 0.05
1315	1.76	0.0243	0.588	0.317	0.412	1.42	5100	0.017 ± 0.001	0.045	0.24 ± 0.02
1325	1.15	0.0103	0.491	0.317	0.412	1.34	6600	0.0122 ± 0.0005	0.016	0.50 ± 0.03
1325	1.34	0.0140	0.526	0.317	0.412	1.98	6600	0.018 ± 0.002	0.023	0.50 ± 0.06
1325	1.76	0.0243	0.588	0.317	0.412	0.87	2400	0.0217 ± 0.0009	0.045	0.32 ± 0.02
1335	1.15	0.0103	0.491	0.317	0.412	1.70	6600	0.0154 ± 0.0004	0.016	0.64 ± 0.04
1335	1.34	0.0140	0.526	0.317	0.412	2.48	6600	0.023 ± 0.002	0.023	0.64 ± 0.06
1335	1.76	0.0243	0.588	0.317	0.412	1.07	2400	0.027 ± 0.001	0.045	0.40 ± 0.02
1350	1.15	0.0103	0.491	0.317	0.412	1.81	5100	0.0213 ± 0.0004	0.016	0.88 ± 0.05
1350	1.34	0.0140	0.526	0.317	0.412	2.65	5100	0.031 ± 0.002	0.023	0.89 ± 0.06
1350	1.76	0.0243	0.588	0.317	0.412	1.18	1800	0.039 ± 0.002	0.045	0.57 ± 0.03
1364	1.15	0.0103	0.491	0.317	0.412	1.47	3000	0.0294 ± 0.0005	0.016	1.23 ± 0.07
1364	1.34	0.0140	0.526	0.317	0.412	2.14	3000	0.043 ± 0.002	0.023	1.23 ± 0.07
1364	1.76	0.0243	0.588	0.317	0.412	1.37	1500	0.055 ± 0.001	0.045	0.82 ± 0.03
1374	1.15	0.0103	0.491	0.317	0.412	1.84	3000	0.0369 ± 0.0006	0.016	1.55 ± 0.08
1374	1.34	0.0140	0.526	0.317	0.412	2.62	3000	0.053 ± 0.002	0.023	1.52 ± 0.08
1374	1.76	0.0243	0.588	0.317	0.412	1.73	1500	0.0689 ± 0.0008	0.045	1.03 ± 0.03
1399	1.15	0.0103	0.491	0.317	0.412	2.47	2400	0.0619 ± 0.0008	0.016	2.6 ± 0.1
1399	1.34	0.0140	0.526	0.317	0.412	3.52	2400	0.088 ± 0.002	0.023	2.6 ± 0.1
1399	1.76	0.0243	0.588	0.317	0.412	1.75	900	0.117 ± 0.002	0.045	1.75 ± 0.06
1421	1.15	0.0103	0.491	0.317	0.412	3.94	2400	0.0987 ± 0.0008	0.016	4.2 ± 0.2
1421	1.34	0.0140	0.526	0.317	0.412	5.71	2400	0.143 ± 0.002	0.023	4.2 ± 0.2
1421	1.76	0.0243	0.588	0.317	0.412	2.84	900	0.189 ± 0.002	0.045	2.87 ± 0.09
1433	1.15	0.0103	0.491	0.317	0.412	3.80	1800	0.1269 ± 0.0007	0.016	5.4 ± 0.3
1433	1.34	0.0140	0.526	0.317	0.412	5.51	1800	0.184 ± 0.002	0.023	5.4 ± 0.2
1433	1.76	0.0243	0.588	0.317	0.412	3.63	900	0.243 ± 0.001	0.045	3.7 ± 0.1
1446	1.15	0.0103	0.491	0.317	0.412	4.95	1800	0.1651 ± 0.0007	0.016	7.1 ± 0.4
1446	1.34	0.0140	0.526	0.317	0.412	7.17	1800	0.239 ± 0.002	0.023	7.1 ± 0.3
1446	1.76	0.0243	0.588	0.317	0.412	6.28	1200	0.314 ± 0.002	0.045	4.8 ± 0.1
1470	1.15	0.0103	0.491	0.317	0.412	9.34	2100	0.267 ± 0.002	0.016	11.6 ± 0.6
1470	1.34	0.0140	0.526	0.317	0.412	13.43	2100	0.384 ± 0.004	0.023	11.4 ± 0.5
1470	1.76	0.0243	0.588	0.317	0.412	7.67	900	0.5109 ± 0.0009	0.045	7.9 ± 0.2
1495	1.15	0.0103	0.491	0.317	0.412	8.45	1200	0.423 ± 0.002	0.016	18.5 ± 0.10
1495	1.34	0.0140	0.526	0.317	0.412	11.78	1200	0.589 ± 0.005	0.023	17.7 ± 0.8
1495	1.76	0.0243	0.588	0.317	0.412	16.38	1200	0.820 ± 0.005	0.045	12.7 ± 0.4
1519	1.15	0.0103	0.491	0.317	0.412	16.64	1500	0.667 ± 0.005	0.016	29 ± 2
1519	1.34	0.0140	0.526	0.317	0.412	22.00	1500	0.88 ± 0.01	0.023	27 ± 1
1519	1.76	0.0243	0.588	0.317	0.412	19.25	900	1.284 ± 0.002	0.045	20.1 ± 0.6

[a] Listed in the table are the run temperature, T/K, the diameter of the cell orifice, d/mm, the area of the effusion orifice, B/cm^2, the Clausing factor for the orifice, W_B, the area of the evaporating surface, A/cm^2 the Clausing factor for the cell, W_A, the total mass lost during the isothermal period, m/mg, the duration of the isothermal period, t/s, the computed loss rate and its estimated uncertainty, $\dot{m}$/(mg·min^{-1}), the factor, f, as given by eq 9 for each cell, and the value of the apparent, measured vapor pressure, P_m/Pa, as given by eq 3 for each run.

Table 2. Evaporation Coefficient, α, Equilibrium Vapor Pressure, P_{eq}/Pa, and Enthalpy of Reaction, $\Delta_{rxn}H°$(298.15 K) /(kJ·mol^{-1}), for SiO Derived from the Measurements Using Three Different Knudsen Cell Orifice Sizes

T/K	α	P_{eq}/Pa	$\Delta_{rxn}H°$(298.15 K)/(kJ·mol^{-1})
1301	0.019 ± 0.008	0.5 ± 0.2	357 ± 3
1315	0.029 ± 0.0010	0.6 ± 0.1	359 ± 2
1325	0.032 ± 0.009	0.8 ± 0.1	359 ± 2
1335	0.029 ± 0.008	1.0 ± 0.1	359 ± 2
1350	0.033 ± 0.008	1.4 ± 0.2	359 ± 1
1364	0.036 ± 0.007	1.9 ± 0.2	360 ± 1
1374	0.036 ± 0.007	2.4 ± 0.2	360 ± 1
1399	0.037 ± 0.007	4.0 ± 0.4	360 ± 1
1421	0.039 ± 0.008	6.3 ± 0.6	360 ± 1
1433	0.038 ± 0.007	8.2 ± 0.7	359 ± 1
1446	0.037 ± 0.007	10.9 ± 0.1	359 ± 1
1470	0.038 ± 0.007	17 ± 2	359 ± 1
1495	0.043 ± 0.008	26 ± 2	359 ± 1
1519	0.047 ± 0.009	40 ± 3	360 ± 1

vapor pressure which they collected using the multiple Knudsen cell mass spectrometric method.[15] The focus of their work was to examine the stability of amorphous SiO by studying the vapor pressure of both commercial $SiO_{(am)}$ powder and the vapor pressure of silicon monoxide over a diphasic mixture of silicon and silica. Ionic intensities from the samples were also compared with a cell loaded with silver. Using cells with different effusion orifices, these authors were able to calculate evaporation coefficients for both the $SiO_{(am)}$ and the Si/SiO_2 mixtures. Over the temperature range (1175 to 1410) K, Rocabois et al. calculated the evaporation coefficient of $SiO_{(am)}$ to range from approximately 0.017 to 0.03 over this temperature range while the evaporation coefficients for the Si/SiO_2 mixture were about an order of magnitude lower. After correcting for these evaporation coefficients, Rocabois et al. concluded that both $SiO_{(am)}$ and the Si/SiO_2 mixtures gave the same vapor pressure, within the uncertainty range in their measurements. Rocabois et al. did not provide individual data points for the evaporation coefficient, publishing only a fit to their data. This fit to their data is shown as the solid line in Figure 4 along with the values measured in this study. The dashed line respresents an extrapolation of the fit from Rocabois et al. above their experimental range. Given the difficulty in measuring this value and the potential for errors, the agreement between the two data sets is quite remarkable. The current values are slightly higher than the Rocabois et al. fit, but agree within the estimated uncertainty in this work. Furthermore, the two data sets seem to exhibit a similar temperature dependence.

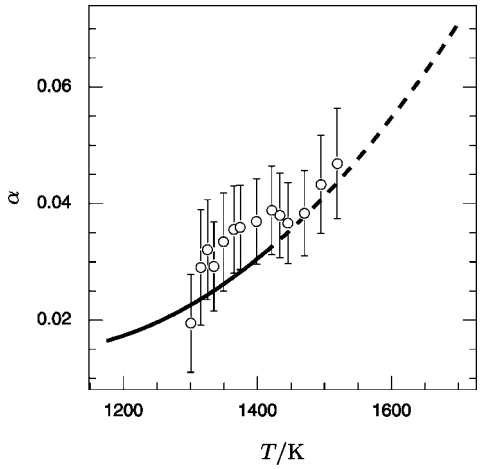

Figure 4. Plot of the calculated evaporation coefficient, α, for SiO taken from the series of vapor pressure measurements with Knudsen cells of different effusion orifice sizes.

The evaporation coefficient arises from a slow step or "bottleneck" in the evaporation process. As noted by Rocabois et al., the larger number of Si−O contacts favor the evaporation kinetics in (nominal) amorphous silicon monoxide, leading to an evaporation coefficient for $SiO_{(am)}$ to be higher than for a mixture of $Si_{(s)}$ and $SiO_{2(s)}$.[15] In 1983, Hashimoto prepared a chondrule analog and then heated this material to various high temperatures under vacuum to measure the loss rate of components such as FeO, MgO, and SiO_2 with time.[28] Fedkin et al. have recently modeled the data from these experiments to estimate, among other quantites, the evaporation coefficient of SiO gas. Fedkin et al. calculated this value to range from 0.12 to 0.21 over the temperature range from (1973 to 2273) K, respectively.[29] Interestingly, a rough extrapolation of the Rocabois et al. expression and the current results appear to be consistent with these results, but it should be emphasized that the evaporation coefficient in this work is for SiO gas over a nominal, amorphous silicon monoxide powder whereas the Fedkin et al. work involves a more complex silicate mixture.

The intercept of the P_m vs ($P_m f$) plot represents an extrapolation to zero orifice area and hence gives the equilibrium vapor pressure. These equilibrium vapor pressures and their associated uncertainty are given in Table 2 and also plotted in Figure 5. With the exception of the lowest temperature data points, the estimated uncertainty in the vapor pressure values are nearly comparable to the symbol size.

A weighted fit to these vapor pressure values as a function of temperature was made and is shown as the solid line in Figure 5. This fit to the equilibrium vapor pressure data was made using the same FITEXY routine described previously and weighting factors as given in eq 12. A constant, ± 5 K uncertainty was used in the temperature while the uncertainties listed in Table 2 were used in the vapor pressure values. This linear fit to the data is

$$\log_{10}(P/\text{Pa}) = (13.29 \pm 0.39) - \frac{(17740 \pm 550)}{T/\text{K}} \quad (13)$$

A comparison of the current experimental data with other works is also given in Figure 5. Unfortunately, as noted in the Introduction, the number of investigations of the reaction in eq 1, the vapor pressure of $SiO_{(g)}$ over the nominal, $SiO_{(am)}$, is rather small. The first measurement of the vapor pressure of SiO was made by Gel'd and Kochnev in 1948.[30] Perhaps because of the metastability of SiO, the data of these authors is often interpreted as belonging to the reaction in eq 2. According to Schnurre, et al., these authors clearly state that they produced amorphous SiO by condensing the vapors according to reaction 2 and then used this product in their Knudsen effusion studies. The data from Gel'd and Kochnev are denoted by the triangles in Figure 5.

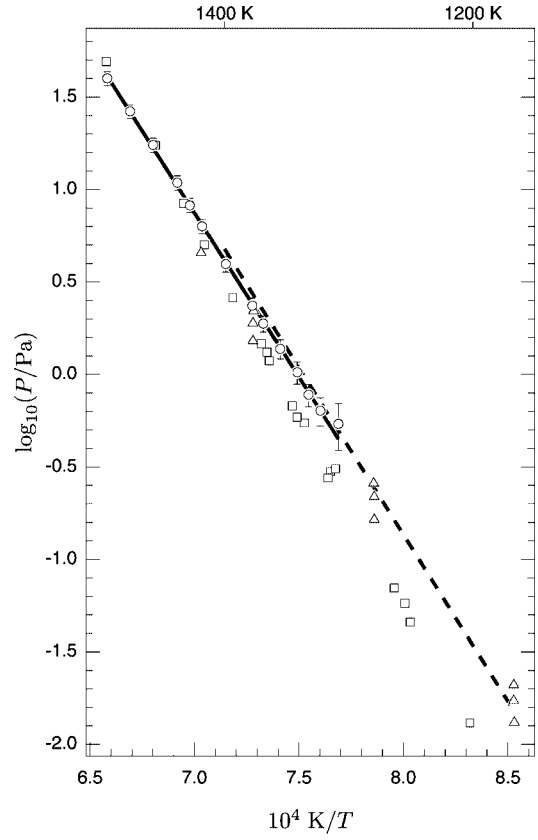

Figure 5. Comparison of available experimental data for $SiO_{(am)}$ evaporation. Shown in the figure are experimental data reported in this work (circles), taken by Gel'd and Kochnev (triangles), and by Gunther (squares) and Rocabois et al. (thick dashed line). A fit to the experimental data taken in this work is given by the solid line.

There is some overlap in the experimental temperature range between the current results and those of Gel'd and Kochnev. The vapor pressure values in this range are nearly the same, but the values in this work are slightly higher than all of the values from Gel'd and Kochnev in this temperature range.

Knudsen effusion data taken by Gunther in 1957 is shown as the squares in Figure 5.[14] These data span a rather large range in temperature, namely (1290 to 1500) K, and the vapor pressure data were taken with several different effusion areas, all of which are shown in Figure 5. The vapor pressure values at the highest temperatures compare favorably with the current work, but the slope of the vapor pressure values is steeper than in the current work.

Individual data points for Rocabois et al. are not available, but the fit to their results for SiO evaporation is shown as the dashed line in Figure 5. Again, the agreement between the current results and those of Rocabois et al. is very good and there is some overlap between the two data sets with a close match in the slope of the vapor pressure data.

As noted in the Introduction, the evaporation of $SiO_{(am)}$ actually corresponds to the reaction given in eq 2 with a mixture of very small domains of Si and SiO_2. It is perhaps important to reiterate a subtle distinction in the thermodynamic treatment that follows on the nominal evaporation of amorphous silicon

monoxide. In some previous works in the literature, eq 1 has been used with thermodynamic properties of the amorphous silicon monoxide assumed to be given by an equimolar mixture of Si and SiO_2. In this work, eq 2 is used. Whereas both treatments would give essentially the same thermodynamic data for the reactants, in this work no assumption is made about the thermodynamic properties of the reactants—they correspond exactly to those given in eq 2. Thermodynamic data for species in eq 2 were taken from ref 24 and a second-law analysis of the vapor pressure has been performed to yield $\Delta_{rxn}H°(298.15\ K) = (351 \pm 11)\ kJ\cdot mol^{-1}$, where the uncertainty in this estimate is due to the uncertainty in the slope of eq 13.

A third-law analysis was performed for each of the equilibrium vapor pressure values given in Table 2 and these values are shown in the fourth column of that table. These values appear to be relatively constant with no noticeable drift with temperature. Uncertainty estimates in individual enthalpy of reaction values in column 4 are based entirely on the uncertainty estimates given for the equilibrium vapor pressure values in the preceding column. Averaging these individual third-law enthalpy values yields $\Delta_{rxn}H°(298.15\ K) = (359.1 \pm 2.0)\ kJ\cdot mol^{-1}$. The second-law value is lower than the third-law result, but the two agree within the experimental uncertainty in both values. Using the third-law value, the enthalpy of formation of $SiO_{(g)}$ can be calculated as $\Delta_f H°(298.15\ K) = (-93.6 \pm 2.0)\ kJ\cdot mol^{-1}$ which compares favorably with the value, $(-96.3 \pm 4.5)\ kJ\cdot mol^{-1}$ reported by Rocabois et al.[15]

Several estimates of the vapor pressure of silicon monoxide have been made in the past based on thermodynamic assessments, some of which have been used extensively in the literature[2−4] and the purpose of this section is to highlight how these assessments compare with the available experimental data. A comprehensive review of the vaporization of silica was made by Schick in 1960.[31] As noted in his work, the primary motivation was to provide data for the temperature range of (2000 to 3000) K. In his article, one section was devoted to the condensation of $SiO_{(g)}$ and in this section, Schick reported an expression for the standard Gibbs energy change of reaction 1 which was initially derived by Brewer and Edwards.[32] In that work, Brewer and Edwards took data collected by Tombs and Welch[33] over the temperature range (1573 to 1920) K, assuming it referred to reaction 1. These data yielded $\Delta H° = 245.0\ kJ\cdot mol^{-1}$, and they estimated the standard entropy change for this reaction to be $\Delta S° = 0.1065\ kJ\cdot mol^{-1}\cdot K^{-1}$, yielding the following equation for the Gibbs energy change over the experimental temperature range:

$$\Delta G°/(kJ\cdot mol^{-1}) = 245.0 - 0.1065(T/K) \qquad (14)$$

A plot of the vapor pressure predicted by this expression is shown over the temperature range (1000 to 2200) K in Figure 6 as the thin solid line. This expression has been extrapolated down to 1000 K to highlight differences in the vapor pressure values at this level. This expression has unfortunately been used often in modeling of silicon monoxide condensation at temperatures of 1000 K or below.[2−4] This plot clearly demonstrates that these extrapolated values are significantly higher than predicted by a similar extrapolation of the current, silicon monoxide vapor pressure data. The problem in this expression lies in the estimated value of the entropy term in eq 14 and in their original work, Brewer and Edwards noted that this term may be in error.[32]

In an attempt to improve this equation, Schick reasoned that the Gibbs energy term given by eq 14 at approximately 2000 K should be close to the true value. Using this value and an improved estimate of the entropy term at 2000 K taken from heat capacity and spectroscopic data, he reformulated the Gibbs energy equation to one more suitable for extrapolation:

$$\Delta G°/(kJ\cdot mol^{-1}) = 324.4 - 0.1462(T/K) \qquad (15)$$

The vapor pressure predicted by this expression is shown as the short dashed line in Figure 6. As mentioned earlier, the two curves interesect at 2000 K, yet with the improved estimate for $\Delta S°$, the extrapolation to lower temperatures appears to be much improved. Interestingly, this expression also tends to agree well with the majority of the experimental data. Schick recommended this expression as the best estimate, but unfortunately the previous expression (now shown to be incorrect) has often been used in the literature instead.[2,4]

In 1967, Kubaschewski et al. reviewed the available data on silicon monoxide. These authors used Gibbs energy of reaction data taken for reaction 2, heat capacity data estimates for gaseous and (nominally) amorphous SiO, and estimates of the standard entropy of $SiO_{(am)}$ to estimate $\Delta_{sub}H°(298.15\ K)$ for SiO as $(333 \pm 25)\ kJ\cdot mol^{-1}$. They also provided the following, computed equation for SiO vapor pressure:

$$\log_{10}(P/Pa) = -\frac{(17750)}{T/K} - 2.77\log_{10}(T/K) + 17.42 \qquad (16)$$

This expression has been plotted in Figure 6 as the dotted line. While this expression is close to the experimental data at the very lowest temperature range, there is a deviation from the experimental data that tends to grow with temperature and

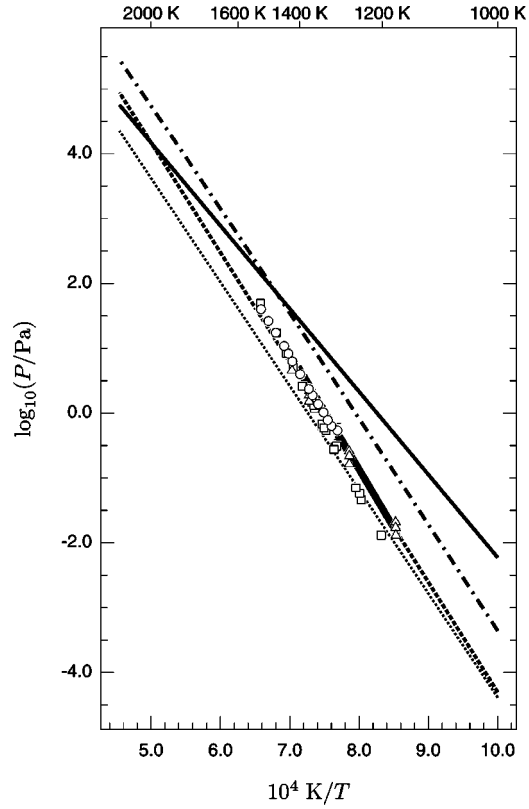

Figure 6. Comparison of the current experimental data for $SiO_{(am)}$ evaporation with thermodynamic assessments of SiO vapor pressure. Shown in the figure are experimental data reported in this work (circles), taken by Gel'd and Kochnev (triangles), and by Gunther (squares) and Rocabois et al. (thick, solid line). Thermodynamic assessments of SiO vapor pressure are shown by Schick (solid line and short dashed line), Kubaschewski (dotted line), and Schnurre et al. (dashed-dotted line).

the expression underestimates the actual vapor pressure.

The most recent assessed value for SiO vapor pressure is given by Schnurre et al.[9] These authors presented a comprehensive study of silicon monoxide and its thermochemical data in an effort to improve the Czochralski (CZ-Si) process of producing large silicon monocrystals. In this process, SiO_2 forms particles which can cause dislocations and inhibit the growth of these crystals. These authors placed a covered tube over a silica melt at 1693 K and measured the distance to the zone of SiO condensation within the tube. This distance was approximately 4 mm, and they estimated the drop in temperature over this range to be (25 to 100) K. On the basis of the metastability of SiO and the results of their condensation experiment, these authors concluded that the vapor pressure of SiO gas over $SiO_{(am)}$ must be higher than the vapor pressure of SiO gas over a mixture of silicon and SiO_2 at the same temperature. Kubaschewski and Chart[34] performed careful experiments on the vapor pressure of SiO over the silicon/silica mixture, and Schnurre et al. noted that these values are higher than the data collected by Gel'd and Kochnev for SiO vapor pressure over amorphous SiO.[9] Therefore, Schnurre et al. rejected the data of Gel'd and Kochnev as being too low. On the basis of the conclusion from their own work that $P_{SiO}^{SiO_{am}} > P_{SiO}^{Si+SiO_2}$ and using other available thermodynamic data on SiO, Schnurre et al. estimated the vapor pressure of silicon monoxide to be the values given by the dotted-dashed line in Figure 6. These values are higher than all of the experimental data in the literature on the nominal, amorphous silicon monoxide evaporation, but their vapor pressure assessment does appear to have a similar slope as the equilibrium vapor pressure data reported in this current work.

Certainly, at the same temperature it seems reasonable to expect that the vapor pressure of silicon monoxide gas should be higher over amorphous silicon monoxide than over a mixture of silicon and silica. Rocabois et al. have argued that if the evaporation coefficients of these two systems are taken into account, then the two systems have essentially identical vapor pressures. The assessment of Schnurre et al. was based on the fact that the vapor pressure of amorphous silicon monoxide must be greater than that of the data taken by Kubaschewski and Chart. In their Knudsen effusion study, Kubaschewski and Chart correctly accounted for the evaporation coefficients, but in the experiment by Schnurre et al., the vapor was allowed to evaporate freely and evaporation coefficients were not considered. This likely is the reason that the assessment by Schnurre et al. is well above the available experimental data and other previous assessments. In addition, it should also be noted that the expression given by Schnurre et al. predicts that the sublimation of SiO occurs at 2070 K and 1 bar, in contrast to the observation that the boiling point of SiO is above 2273 K.[35]

7. Summary

Because of the lack of experimental data and its importance to a variety of fields, we have measured the vapor pressure of (nominally) amorphous, silicon monoxide. These data appear to be in reasonable agreement with other sources of experimental data on silicon monoxide vapor pressure. Evaporation coefficients for amorphous silicon monoxide were measured as approximately 0.02 to 0.05 over the temperature range of (1301 to 1519) K and these values for the evaporation coefficient agree quite closely with previous measurements of this quantity. The enthalpy of reaction at 298.15 K for the vaporization reaction was calculated via second- and third-law analyses as (351 ± 11) and (359.1 ± 2.0) $kJ \cdot mol^{-1}$, respectively. A comparison of the experimental vapor pressure data and expressions for the vapor pressure based on thermodynamic assessments was made. One additional result of this work is that an expression for the vapor pressure of silicon monoxide that is often used in astrophysical literature has been shown to greatly overpredict the vapor pressure of silicon monoxide in the temperature range where it typically is used.

Literature Cited

(1) Han, S.; Grozea, D.; Huang, C.; Lu, Z. H. Al:SiO thin films for organic light-emitting diodes. *J. Appl. Phys.* **2004**, *96*, 709–714.
(2) Nuth, J. A.; Donn, B. Experimental Studies of the Vapor Phase Nucleation of Refractory Compounds. I. The condensation of SiO. *J. Chem. Phys.* **1982**, *77*, 2639–2646.
(3) Nuth, J. A.; Donn, B. Experimental Studies of the Vapor Phase Nucleation of Refractory Compounds. II. The Condensation of an Amorphous Magnesium Silicate. *J. Chem. Phys.* **1983**, *78*, 1618–1620.
(4) Gail, H.-P.; Sedlmayr, E. Mineral formation in stellar winds I. Condensation sequence of silicate and iron grains in stationary oxygen rich outflows. *Astron. Astrophys.* **1999**, *347*, 594–616.
(5) Jeong, K. S.; Winters, J. M.; Bertre, T.; Le.; Sedlmayr, E. Self-consistent modeling of the outflow from the O-rich Mira IRC-20197. *Astron. Astrophys.* **2003**, *407*, 191–206.
(6) Hertl, W.; Pultz, W. W. Disproportionation and Vaporization of Solid Silicon Monoxide. *J. Am. Ceram. Soc.* **1967**, *50*, 378–381.
(7) Kubaschewski, O.; Evans, E. L.; Alcock, C. B. *Metallurgical Thermochemistry*; Pergamon Press: London, 1967.
(8) Nagamori, M.; Boivin, J.-A.; Claveau, A. Gibbs free energies of formation of amorphous Si_2 O_3, SiO and Si_2 O. *J. Non-Cryst. Solids* **1995**, *189*, 270–276.
(9) Schnurre, S. M.; Gröbner, J.; Schmid-Fetzer, R. Thermodynamics and phase stability in the Si-O system. *J. Non-Cryst. Solids* **2004**, *336*, 1–24.
(10) Philipp, H. R. Optical Properties of Non-crystalline Si, SiO, SiO_x and SiO_2. *J. Phys. Chem. Solids* **1971**, *32*, 1935–1945.
(11) Brady, G. W. A Study of Amorphous SiO. *J. Phys. Chem.* **1959**, *63*, 1119–1120.
(12) Hohl, A.; Wider, T.; van Aken, P. A.; Weirich, T. E.; Genninger, G.; Vidal, M.; Oswald, S.; Deneke, C.; Mayer, J.; Fuess, H. An interface clusters mixture model for the structure of amorphous silicon monoxide (SiO). *J. Non-Cryst. Solids* **2003**, *320*, 255–280.
(13) Friede, B.; Jansen, M. Some comments on so-called 'silicon monoxide'. *J. Non-Cryst. Solids* **1996**, *204*, 202–203.
(14) Gunther, K. G. On the measurement of the vapor pressure and evaporation rate of glass-forming substances. *Glastech. Ber.* **1958**, *31*, 9–15.
(15) Rocabois, P.; Chatillon, C.; Bernard, C. Vapor pressure and evaporation coefficient of SiO (amorphous) and $SiO_{2\ (s)} + Si_{(s)}$ mixtures by the multiple Knudsen cell mass spectrometric method. *Rev. Int. Hautes Temper. Refract.* **1992**, *28*, 37–48.
(16) Ferguson, F. T.; Gardner, K. G.; Nuth, J. A. The Vapor Pressure of Palladium from 1473 to 1973 K. *J. Chem. Eng. Data* **2006**, *51*, 1509–1515.
(17) Ferguson, F. T.; Nuth, J. A.; Johnson, N. M. Thermogravimetric Measurement of the Vapor Pressure of Iron from 1573 to 1973 K. *J. Chem. Eng. Data* **2004**, *49*, 497–501.
(18) Clausing, P. The Flow of Highly Rarefied Gases through Tubes of Arbitrary Length. *Vac. Sci. Technol.* **1971**, *8*, 636–756.
(19) Berman, A. S. Free Molecule Transmission Probabilities. *J. Appl. Phys.* **1965**, *10*, 3356.
(20) Szwemin, P.; Niewiński, M. Comparison of transmission probabilities calculated by Monte Carlo simulation and analytical methods. *Vacuum* **2002**, *67*, 359–362.
(21) Drowart, J.; Chatillon, C.; Hastie, J.; Bonnell, D. High-Temperature Mass Spectrometry: Instrumental Techniques, Ionization Cross-sections, Pressure Measurements, and Thermodynamic Data. *Pure Appl. Chem.* **2005**, *77*, 693–737.
(22) Whitman, C. On the Measurement of Vapor Pressures by Effusion. *J. Chem. Phys.* **1952**, *20*, 161–164.
(23) Motzfeldt, K. The Thermal Decomposition of Sodium Carbonate by the Effusion Method. *J. Phys. Chem.* **1955**, *59*, 139–147.
(24) Chase, M. W., Jr. *NIST-JANAF Thermochemical Tables*; American Institute of Physics: New York, 1998.
(25) Winterbottom, W. L.; Hirth, J. P. Diffusional Contribution to the Total Flow from a Knudsen Cell. *J. Chem. Phys.* **1962**, *37*, 784–793.

(26) Ward, J. W.; Bivins, R. L.; Fraser, M. V. Monte Carlo Simulation of Specular and Surface Diffusional Perturbations to Flow from Knudsen Cells. *J. Vac. Sci. Technol.* **1969**, *7*, 206–210.

(27) Press, W. H.; Teukolsky, S. A.; Vetterling, W. T.; Flannery, B. P. *Numerical Recipes in C*; Cambridge University Press: Cambridge, UK, 1992.

(28) Hashimoto, A. Evaporation metamorphism in the early solar nebula-evaporation experiments on the melt FeO-MgO-SiO_2-CaO-Al_2 O_3 and chemical fractionations of primitive materials. *Geochem. J.* **1983**, *17*, 111–145.

(29) Fedkin, A. V.; Grossman, L.; Ghiorso, M. S. Vapor pressures and evaporation coefficients for melts of ferromagnesian chondrule-like compositions. *Geochim. Cosmochim. Acta* **2006**, *70*, 206–223.

(30) Gel'd, P. V.; Kochnev, M. J. Equilibria of systems involving silicon monoxide. *Zh. Prikl. Khim.* **1948**, *21*, 1249–1260.

(31) Schick, H. L. A Thermodynamic Analysis of the High-Temperature Vaporization Properties of Silica. *Chem. Rev.* **1960**, *60*, 331–362.

(32) Brewer, L.; Edwards, R. K. The Stability of SiO Solid and Gas. *J. Phys. Chem.* **1954**, *58*, 351–358.

(33) Tombs, N. C.; Welch, A. J. E. Thermodynamic Properties of Silicon Monoxide. *J. Iron Steel Inst.* **1952**, *172*, 69–78.

(34) Kubaschewski, O.; Chart, T. G. Silicon monoxide pressures due to the reaction between solid silicon and silica. *J. Chem. Thermodyn.* **1974**, *6*, 467–476.

(35) Filsinger, D. H.; Bourrie, D. B. Silica to Silicon: Key Carbothermic Reactions and Kinetics. *J. Am. Ceram. Soc.* **1990**, *73*, 1726–1732.

Received for review July 18, 2008. Accepted September 28, 2008.

JE800560B